

DOI: 10.51981/2588-0039.2023.46.022

MAGNETIC FIELD CONFIGURATIONS AT SOLAR FLARE SITES ABOVE ACTIVE REGION AR 10365 FROM MHD SIMULATION RESULTS

A.I. Podgorny¹, I.M. Podgorny²

¹*Lebedev Physical Institute RAS, Moscow, Russia; e-mail: podgorny@lebedev.ru*

²*Institute of Astronomy RAS, Moscow, Russia*

Abstract. The fast release of the magnetic energy of the current sheet leads to the observed manifestations of the flare, which are explained by the electrodynamic model of the flare proposed by I. M. Podgorny. The study of the solar flare mechanism by the magnetohydrodynamic (MHD) simulation in the solar corona above the real active region is continued. Two variants of calculation were carried out for relatively high viscosities ($Re_m=3\times 10^4$, $Re=10^4$) and for low viscosities ($Re_m=10^9$, $Re=10^7$). For MHD simulations with high viscosities, a property was found that is possessed only by those current density maxima that are located in the bright region of pre-flare radio.

Introduction

The primordial release of magnetic energy during solar flares occurs in the solar corona above the active region at altitudes of 15 - 70 Mm, which is proven by both direct observations of thermal X-ray emission from flares on the limb [1] and analysis of flare observation data [2-4].

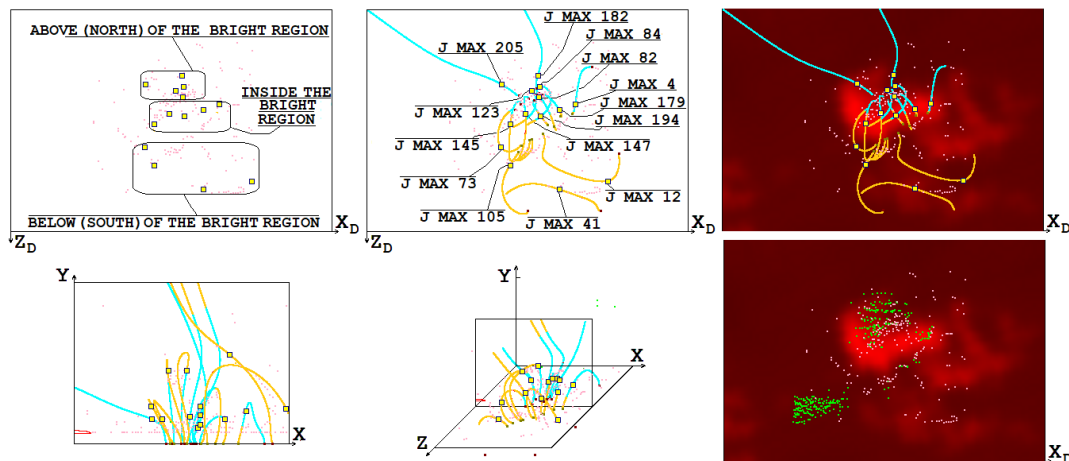


Figure 1. Comparison of the magnetic field configuration and the positions of the current density maxima with the distribution of radio emission intensity at a frequency of 17 GHz on May 26, 2003 at 02:32:05 three hours before the M 1.9 flare for calculation with relatively high viscosities ($Re_m=3\times 10^4$, $Re=10^4$). The positions of the current density maxima are shown as violet points. The magnetic field configuration is presented by magnetic lines which pass through selected current density maxima with numbers 4, 12, 41, 73, 82, 84, 105, 123, 145, 147, 179, 182, 194, 205. 3D magnetic lines in the computational domain and their projections onto the picture plain (which is perpendicular to line of sight direction) and onto the central plane of computation domain are shown. In the lower right corner, the current density maxima for calculations with two sets of viscosities (violet dots and green dots) are presented.

The appearance of flares in the corona is explained by the mechanism of S.I. Syrovatsky [5], according to which the flare energy accumulates in the magnetic field of the current sheet. A current sheet is formed in the vicinity of a singular magnetic field line under the influence of disturbances propagating from the solar surface. During quasi-stationary evolution the current sheet transfers into an unstable state (see, for example, [6]). The flare release of the magnetic field energy of the current sheet as a result of instability leads to the observed manifestations of the flare, which are explained by the electrodynamic model of the solar flare proposed by I. M. Podgorny [7]. Hard beam X-ray radiation on the solar surface appears due to the deceleration in the lower dense layers of the solar atmosphere of electrons accelerated in field-aligned currents on magnetic lines exiting from the current sheet. Field-aligned currents are generated by the Hall electric field in the current sheet. The model was developed based on the results of

observations and numerical magnetohydrodynamics (MHD) simulations and uses analogies with the substorm electrodynamic model proposed earlier by its author [8]. Since it is impossible to determine the configuration of the magnetic field in the corona from observations, to study the physical mechanism of a solar flare it is necessary to carry out MHD simulation of the flare situation in the solar corona above the real active region [9-16], which is continued in this work. When setting up the MHD simulation problem, no assumptions were made about the mechanism of the solar flare; all conditions were taken from observations.

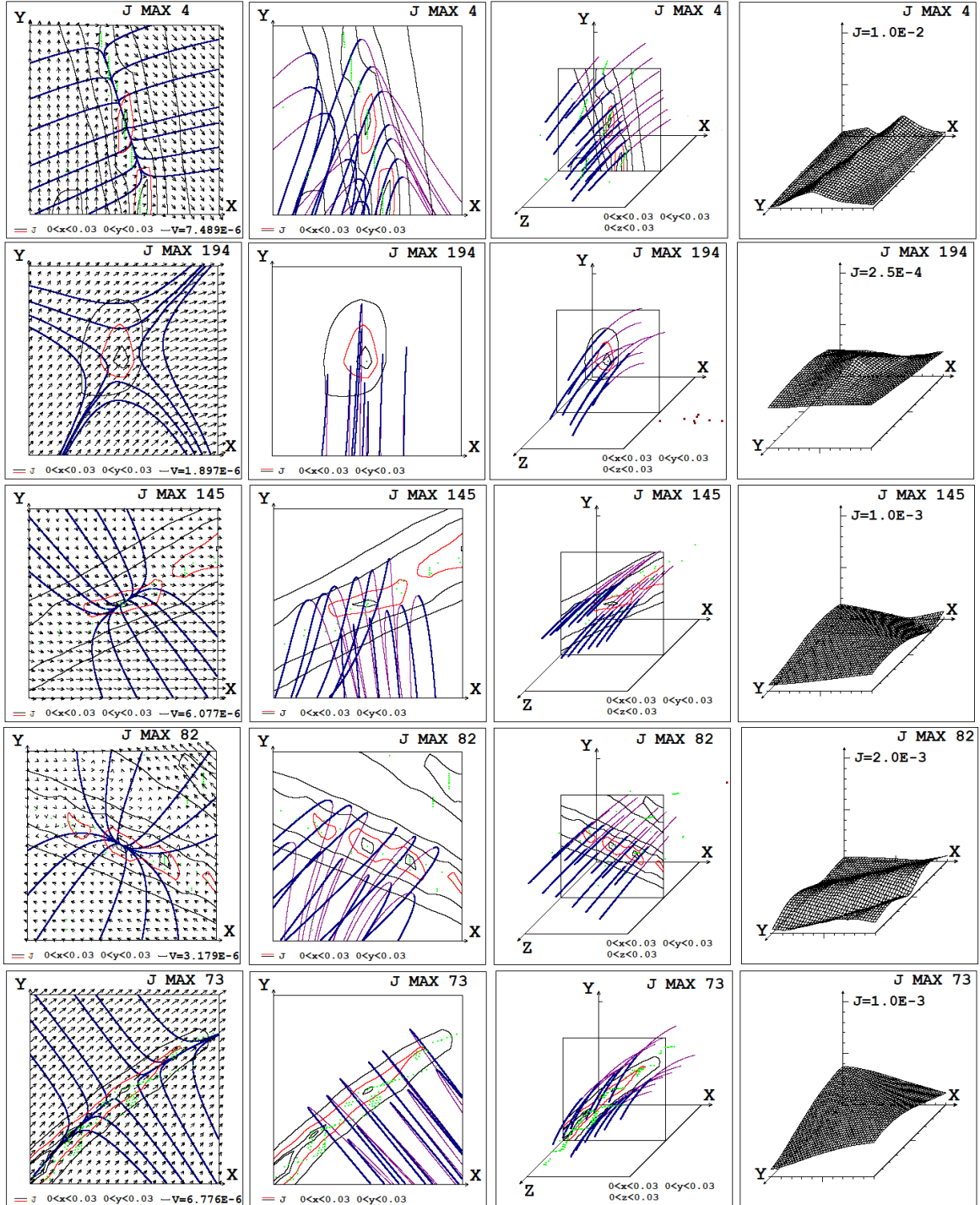


Figure 2. The configurations of the magnetic field, plasma flow velocity, and current density distributions near the selected 4th, 194th, 145th, 82nd, and 73rd current density maxima on May 26, 2003 at 02:32:05 for calculation with relatively high viscosities ($Re_m=3 \times 10^4$, $Re=10^4$) are presented. The configurations are shown by plane magnetic lines which are tangential to projections of magnetic vectors on the plane of configuration, by projections of magnetic lines on the plane of configuration, and by 3D magnetic lines. Magnetic lines located in front of the plane of configuration are shown as bold blue lines, and magnetic lines located behind the plane of configuration are shown as thin brown lines.

Setting of the problem, method of solving the problem, selection of parameters

MHD simulation is carried out above the active region of AR 10365. The computational domain in the corona is a rectangular parallelepiped ($0 \leq x \leq 1$, $0 \leq y \leq 0.3$, $0 \leq z \leq 1$) (the length unit was chosen $L_0 = 4 \times 10^{10}$ cm). The lower boundary of the computational domain $y=0$ (XZ) is located on the surface of the Sun. The Y axis is directed from the Sun perpendicular to the photosphere. The X axis is directed from east to west; the Z axis is from north to south.

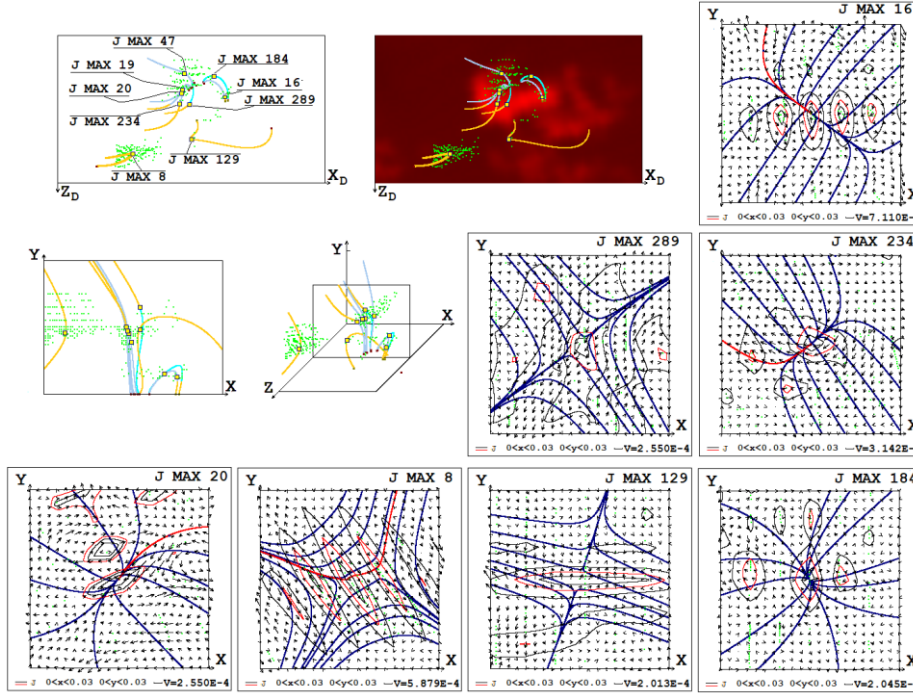


Figure 3. Comparison of the magnetic field configuration and the positions of the current density maxima (green dots) with the distribution of radio emission intensity at a frequency of 17 GHz on May 26, 2003 at 02:32:05 for calculation with relatively low viscosities ($Re_m=10^9$, $Re=10^7$) is shown, as well as in Figure 1. The magnetic configurations near the selected current density maxima are presented.

For the numerical solution, an upwind, absolutely implicit finite-difference scheme was developed which is conservative with respect to the magnetic flux [13, 17]. The scheme was realized in the computer program PERESVET. The simulations were carried out by means of parallel computing threads on graphics cards using CUDA technology [14]. The methods have been developed to stabilize numerical instabilities arise near the boundary [12, 15]. The configuration of the magnetic field obtained by MHD simulation is so complex that it is impossible to determine the positions of singular lines and the current sheets near them from it. For this purpose, a graphical search system of flare positions has been developed [9, 10]. The system is based on the search for current density maxima, which are reached in the middle of the current sheets. The current density maxima are located on singular lines of the magnetic field. To select dimensionless parameters the principle of limited simulation [18] was used. Two variants of calculation were carried out for relatively high magnetic and ordinary viscosities ($Re_m=3 \times 10^4$, $Re=10^4$) and for relatively low viscosities ($Re_m=10^9$, $Re=10^7$). In the first variant, numerical instabilities practically did not arise. At low viscosities, the disturbance propagating from the solar surface is not suppressed.

Results of MHD simulation

Figures 1 - 3 present the results of MHD simulation and their comparison with observations of radio emission at a frequency of 17 GHz in the active region of AO 10365, obtained with the Nobeyama radioheliograph. The results are presented at 02:32:05 on May 6, 2003, three hours before the M 1.9 flare. At this moment, the energy for the flare is accumulated in the magnetic field of the solar corona and the plasma is heated by the currents that create this field. Plasma heated to 6-7 MK causes pre-flare radiation, which can be used to determine the location where the flare will occur in the future.

Figure 1 shows the location of the current density maxima at the time of 02:32:05 on May 6, 2003 for the first calculation variant with relatively high viscosities ($Re_m=3 \times 10^4$, $Re=10^4$). The magnetic field configuration is represented by magnetic lines passing through the selected 14 maxima, indicated by yellow squares, the remaining current density maxima are indicated by violet dots. Superimposed on the configuration of the magnetic field with the positions of the current density maxima in the picture plane (perpendicular to the line of sight) is the distribution of radio emission intensity at a frequency of 17 GHz. The magnetic field configurations near the current density maxima,

which should be located on singular magnetic lines and are places where the magnetic energy of a solar flare is accumulated, are shown in Figure 2 for some selected maxima. Figure 3 shows the location of the current density maxima and magnetic field configuration superimposed on the distribution of radio emission intensity distribution at a frequency of 17 GHz for the second calculation variant with low viscosities ($Re_m=10^9$, $Re=10^7$).

Field configurations near current density maxima (Fig. 2-3) show that a diverging magnetic field is superimposed on an X-type magnetic field (see also [12]). But even the if the superposition is dominated by a divergent magnetic field, due to the presence of the X-type field, a fairly powerful current sheet can appear, as can be seen in the field configuration near the maximum current density No. 82 in Figure 3.

Discussion

Most effectively, the formation of a current sheet occurs for the second variant of the calculation, in which the diffusion spreading is significantly weakened. It can be seen for the current density distribution in the form of a thin sheet for the 129th maximum current density in Figure 3). However, for the second variant ($Re_m=10^9$, $Re=10^7$) the solution is distorted by numerical instabilities: unreal maxima of the current density at points of the numerical grid near the found maximum (Figure 3 for the 8th, 16th, 20th and 234th maxima). As can be seen from Figures 1, 3, a significant part of the current density maxima is located in the bright radiation region. This confirms the solar flare mechanism, based on the accumulation of energy in the magnetic field of the current sheet.

It should be emphasized that in the first variant of the calculation, only the maxima with special property are placed in bright region of preflare emission, and maxima with such properties do not appear outside the bright radiation region. According to this property, current density maximum must be placed in extended (about several tens Mm) current sheet which contain the chain of maxima, and simultaneously the magnetic "plane" lines exiting from the point of maximum must be close to straight line, which means that divergent magnetic field do not dominate strongly. Examples of such an extended current sheet with several maxima are the configuration near the 4th and 145th maxima, presented in Figure 2; the positions of these maxima are presented in Figure 1. The 147th maximum belongs to the same chain as the 145th maximum. For the 82nd maximum (Fig. 2), located in an extended current sheet outside the bright radiation region, "plane" magnetic lines have the shape of parabolas extending from the point of maximum current density, which means, that divergent magnetic field is strongly dominant.

Conclusions

1. A technique has been developed for MHD simulation of a flare situation in the solar corona above an active region and for analyzing the results of MHD simulation which should be improved according the plan developed on the base of obtained results.
2. The location of a large number of current density maxima in the region of bright flare radiation on the solar disk confirms solar flare mechanism, based on the release of energy accumulated in the magnetic field of current sheet.
3. The problem of the formation of a significant number of current sheet maxima outside the bright region of flare radiation is necessary to be solved by improving the MHD simulation technique.
4. It will be necessary to try to use the appearance of configurations with lines close to straight lines along one of the axes in the vicinity of maxima located in the form of chains in an extended current sheet as a precursor for predicting a flare situation obtained from the results of MHD simulation.

The results obtained here are presented more clearly in extended versions of the article in Russian and English posted at the addresses <https://sites.lebedev.ru/ru/podgorny/file/6991> and <https://sites.lebedev.ru/ru/podgorny/file/6992> (Podgorny-Proc-Apatity-2023-Rus_Extended.doc and Podgorny-Proc-Apatity-2023-Eng_Extended.doc at <https://sites.lebedev.ru/ru/podgorny/4171.html>).

References

1. Lin R.P., Krucker S., Hurford G.J. et al. (2003) *Astrophys. J.* 595, L69-L76. <https://doi.org/10.1086/378932>
2. Podgorny A.I., Podgorny I.M., Meshalkina N.S. (2015) *Astron. Rep.* 59, 795–805.
3. Podgorny I.M., Podgorny A.I. (2018) *Astron. Rep.* 62, 696–704.
4. Podgorny I.M., Podgorny A.I. (2019) *Sun and Geosphere* 14(1), 13-76.
5. Syrovatskii S.I. (1966) *Zh. Eksp. Teor. Fiz.* 50, 1133–1147.
6. Podgorny A.I., Podgorny I.M. (2012) *Geomagn. Aeron. (Engl. Transl.)* 52, 150–161.
7. Podgorny I.M., Balabin Y.V., Vashenyuk E.V., Podgorny A.I. (2010) *Astron. Rep.* 54, 645–656.
8. Podgorny I.M., Dubinin E.M., Israilevich P.L., Nicolaeva N.S. (1988) *Geophys. Res. Lett.* 15, 1538–1540.
9. Podgorny A.I., Podgorny I.M. (2013) *Sun and Geosphere* 8(2), 71-76.
10. Podgorny A.I., Podgorny I.M. (2013) *Proc. 36 Annual Sem. "Phys. of Auroral Phenomena"*. Apatity. 117-120.
11. Podgorny A.I., Podgorny I.M., Meshalkina N.S. (2018) *JASTP*, 180, 16-25.
12. Podgorny A.I., Podgorny I.M., Borisenko A.V. (2022) *Open Astronomy*. 31. 27–37.
13. Podgorny A.I., Podgorny I.M., Borisenko A.V. (2023) *Physics* 5(3), 895-910.
14. Podgorny A.I., Podgorny I.M., Borisenko A.V. (2020) *Proc. 43 Annual Sem. "Phys. of Auroral Phenomena"*, Apatity. 56-59.
15. Podgorny A.I., Podgorny I.M., Borisenko A.V. (2021) *Proc 44 Annual Sem. "Phys. of Auroral Phenomena"*, Apatity. 92-95.
16. Podgorny A.I., Podgorny I.M., Borisenko A.V. (2022) *Proc 45 Annual Sem. "Phys. of Auroral Phenomena"*, Apatity. 70-73.
17. Podgorny A.I., Podgorny I.M. (2004) *Comput. Math. Math. Phys.* 44, 1784-1806.
18. Podgorny I.M. (1978) *Simulation studies of Space. Fundamentals of Cosmic Physics* 1, 1-72.